Cell

A Complex Containing PGRL1 and PGR5 Is Involved in the Switch between Linear and Cyclic Electron Flow in *Arabidopsis*

Giovanni DalCorso,[1] Paolo Pesaresi,[2] Simona Masiero,[3] Elena Aseeva,[1] Danja Schünemann,[4] Giovanni Finazzi,[5] Pierre Joliot,[5] Roberto Barbato,[6] and Dario Leister[1,*]

[1]Lehrstuhl für Botanik, Department Biologie, Ludwig-Maximilians-Universität, Menzinger Str. 67, 80638 München, Germany
[2]Dipartimento di Produzione Vegetale, Università Statale di Milano c/o Parco Tecnologico Padano Via Einstein, Loc. Cascina Codazza, 26900 Lodi, Italy
[3]Dipartimento di Biologia, Università degli studi di Milano, Via Celoria 26, 20133 Milan, Italy
[4]Lehrstuhl für Allgemeine und Molekulare Botanik, Ruhr-Universität-Bochum, Gebäude ND 6, 44780 Bochum, Germany
[5]Institut de Biologie Physico-Chimique/UMR-CNRS 7141, 13, rue Pierre et Marie Curie, 75005 Paris, France
[6]Dipartimento di Scienze e Tecnologie Avanzate, Università del Piemonte Orientale, 'Amedeo Avogadro', Corso Borsalino 54, 15100 Alessandria, Italy
*Correspondence: leister@lrz.uni-muenchen.de
DOI 10.1016/j.cell.2007.12.028

SUMMARY

During photosynthesis, two photoreaction centers located in the thylakoid membranes of the chloroplast, photosystems I and II (PSI and PSII), use light energy to mobilize electrons to generate ATP and NADPH. Different modes of electron flow exist, of which the linear electron flow is driven by PSI and PSII, generating ATP and NADPH, whereas the cyclic electron flow (CEF) only generates ATP and is driven by the PSI alone. Different environmental and metabolic conditions require the adjustment of ATP/NADPH ratios and a switch of electron distribution between the two photosystems. With the exception of PGR5, other components facilitating CEF are unknown. Here, we report the identification of PGRL1, a transmembrane protein present in thylakoids of *Arabidopsis thaliana*. Plants lacking PGRL1 show perturbation of CEF, similar to PGR5-deficient plants. We find that PGRL1 and PGR5 interact physically and associate with PSI. We therefore propose that the PGRL1-PGR5 complex facilitates CEF in eukaryotes.

INTRODUCTION

During photosynthesis, light energy is utilized by two spatially separated photoreaction centers located in the thylakoid membranes of the chloroplast, photosystems I (PSI), and II (PSII), to mobilize electrons and ultimately to synthesize ATP and NADPH. Three modes of photosynthetic electron transport exist: in noncyclic (or linear) electron flow (LEF) from water to $NADP^+$ and in pseudocyclic electron flow (PEF) (or "water-water cycle") from water to molecular oxygen PSII and PSI operate in series, while cyclic electron flow (CEF) is driven by PSI alone (reviewed in Allen, 2003). LEF, PEF, and CEF are coupled to the generation of a transthylakoid proton gradient (ΔpH) that drives ATP synthesis, but only LEF produces NADPH. Because the ratio of ATP/NADPH needs to be adjusted to match changing metabolic and photoprotective demands, regulation of the distribution of electrons between LEF and CEF, and thus between the two photosystems, is important for effective photosynthesis (Vallon et al., 1991; Niyogi, 1999; Kramer et al., 2004). CEF operates efficiently in cyanobacteria, in unicellular algae, and in certain tissues of C4 plants (Herbert et al., 1990; Asada et al., 1993; Ravenel et al., 1994; Mi et al., 1995; Finazzi et al., 1999). Earlier studies had suggested that CEF is rather insignificant in C3 plants during steady-state photosynthesis (Herbert et al., 1990; Harbinson and Foyer, 1991; Havaux et al., 1991; Bendall and Manasse, 1995; Joet et al., 2002), but more recent work implies that CEF might contribute substantially to photosynthetic electron flow, at least under certain conditions, for instance during induction of photosynthesis and under stressful conditions like drought, high light, or low CO_2 (Clarke and Johnson, 2001; Joliot and Joliot, 2002, 2006; Golding and Johnson, 2003; Golding et al., 2004).

LEF also requires the membrane-bound cytochrome b_6/f complex (Cyt b_6/f), as well as the mobile electron carriers plastoquinone (PQ), plastocyanin (Pc), and ferredoxin (Fd). CEF shares some components with LEF (PQ, Cyt b_6/f, Pc, PSI, and Fd) and starts with light-dependent excitation of P_{700}, the primary electron donor of PSI, and eventually results in electron transfer to Fd. Oxidized P_{700}^+ is then reduced by electrons from the PQ pool via Cyt b_6/f and Pc. To complete the cycle, electrons from Fd must eventually be donated to PQ. There are two principal routes for this. The NAD(P)H-dehydrogenase (NDH)-dependent pathway plays a major role in cyanobacteria and in certain tissues of C4 plants (Mi et al., 1994; Takabayashi et al., 2005), but its contribution in C3 plants is still ambiguous (Burrows et al., 1998; Havaux et al., 2005; Rumeau et al., 2005; Nandha

et al., 2007). The Fd-dependent pathway (or "CEF around PSI") bypasses NADPH and may play a major role in the acidification of the thylakoid lumen of C3 plants (Munekage et al., 2002, 2004). This ΔpH should in turn contribute to the downregulation of PSII by nonphotochemical quenching (NPQ), the thermal dissipation of excess light energy absorbed by PSII (reviewed in Niyogi, 1999; Shikanai, 2007). It is still not clear whether Fd reduces PQ via Cyt b_6f (Zhang et al., 2001; Kurisu et al., 2003; Stroebel et al., 2003; Joliot et al., 2004; Joliot and Joliot, 2006; Kramer et al., 2004) or directly by means of a Fd:PQ reductase (FQR) (Moss and Bendall, 1984; Cleland and Bendall, 1992; Okegawa et al., 2005) that has not yet been isolated. The CEF/LEF ratio is thought to be modulated by competition between CEF and LEF for reduced Fd, with the relative rates of the two processes being determined by the chloroplast redox poise, and in particular by the balance between PSI donor and acceptor redox states (Joliot and Joliot, 2002; Kramer et al., 2004). A highly active Calvin cycle should form an efficient sink for electrons from PSI and thus favor LEF, whereas CEF will predominate when the dark reactions of photosynthesis are downregulated—for instance, during dark-to-light transitions or under conditions of environmental stress (Breyton et al., 2006). Under conditions of low ATP supply, CEF alone might not suffice to activate LEF. In fact, PEF is thought to restore the redox poise when the electron transport chain is overreduced, thereby activating CEF, which in turn generates the ΔpH and extra ATP for the Calvin cycle to oxidize NADPH (reviewed in Allen, 2003).

Reductions in induced NPQ should therefore accompany defects in CEF. Indeed, a previous screen for *Arabidopsis* mutants that show decreased NPQ identified the small thylakoid protein PGR5, which is involved in Fd-dependent CEF (Munekage et al., 2002). The *crr2 pgr5* double mutant defective in both NDH- and Fd-dependent CEF shows very retarded growth, suggesting that CEF around PSI is always essential for efficient photosynthesis in C3 plants (Munekage et al., 2004). However, the molecular function of PGR5 and the regulation of the switch between CEF and LEF in C3 plants remain unclear.

Here we show that the thylakoid transmembrane protein PGRL1 represents a novel component of Fd-dependent CEF, interacting functionally and physically with PGR5 in *Arabidopsis*. Our data suggest that a PGRL1-PGR5 complex transiently interacts with PSI and Cyt b_6f to allow efficient CEF around PSI.

RESULTS

PGRL1 Is an Integral Thylakoid Protein

Groups of transcriptionally coregulated nuclear genes (regulons) in *Arabidopsis thaliana* that were enriched for photosynthetic genes have been previously identified (Biehl et al., 2005). These photosynthetic regulons include genes of unknown function, the products of which represent putative photosynthetic proteins. One of these, designated PGRL1 (because of its *pgr5*-like photosynthetic phenotype; see below), is encoded by the two highly homologous genes *At4g22890* (*PGRL1A*) and *At4g11960* (*PGRL1B*) (Figure 1), which are located in segmentally duplicated regions of the *A. thaliana* genome. Genes for *PGRL1* homologs exist in the nuclear genomes of algal and plant species, but not in prokaryotes. All PGRL1 proteins share a predicted N-terminal chloroplast transit peptide, two predicted transmembrane domains (TMs) separated by a loop of 19 amino acids, and a stretch of negatively charged amino acids in the N-terminal loop of the mature protein (Figure 1).

Both *Arabidopsis* isoforms of the protein, PGRL1A and B, are located in the chloroplast, as shown by in vivo subcellular localization of full-length N-terminal fusions to the dsRED protein and by the uptake into chloroplasts of PGRL1A and PGRL1B translated in vitro, with concomitant removal of their transit peptides (Figures 2A and 2B; Supplemental Experimental Procedures available online). Chloroplast subfractionation after import revealed that both isoforms are thylakoid proteins (Figure 2C). PSII-O is a peripheral, lumen-exposed thylakoid protein and can be released by treatment of thylakoid membranes with urea. Under such conditions, PGRL1 translated in vitro remains predominantly associated with the membrane fraction (Figure 2D), indicating that it is an integral thylakoid protein, as already suggested by the presence of TMs (see Figure 1).

To determine the topology of PGRL1 more precisely (Figure 2E), thylakoids were subjected to mild digestion with trypsin, such that only the stroma-exposed face was accessible to the protease. As expected, PSII-O on the lumen side of the thylakoid membrane was not affected, whereas multiple proteolytic fragments of PGRL1 were detected (Figure 2F). Because the N- and C-terminal parts of PGRL1, but not the loop between the TM domains, contain trypsin cleavage sites, *Topology 1* depicted in Figure 2E represents the actual topology of PGRL1. The appearance of two unexpected, larger fragments might indicate that certain domains of PGRL1 are relatively more resistant to trypsin, perhaps implying tight interactions of PGRL1 with other stroma-exposed thylakoid proteins. Indeed, when protein complexes were released from the thylakoid membrane by treatment of thylakoids with β-dodecylmaltoside prior to exposure to trypsin, both PSII-O and PGRL1 were completely degraded (Figure 2G). The topology of the endogenous *Arabidopsis* PGRL1 protein was also examined by immunoblotting. A PGRL1-specific antiserum raised against the first 140 N-terminal amino acids of the mature protein (see Figure 1) failed to detect PGRL1 in trypsin-treated membranes (Figure 2H), confirming that its N-terminal region is exposed to the stroma.

Mutants Lacking PGRL1 Are Impaired in Photosynthesis

Insertion mutants for *PGRL1A* and *PGRL1B* were obtained from publicly available T-DNA insertion collections (Figure 3A), and each lacked the respective transcript (Figure 3B). The *pgrl1a pgrl1b* double mutant (*pgrl1ab*) was generated by crossing single *pgrl1a* and *pgrl1b* knockouts and screening the resulting F2 generation for homozygous double mutants. All single mutants retained varying amounts of PGRL1 protein derived from the nonmutated *PGRL1* locus (Figure 3C), and they were indistinguishable from the wild-type (WT) with respect to their developmental behavior (Figures 3D and 3E). The *pgrl1ab* double mutant entirely lacked *PGRL1* transcripts and the PGRL1 protein, grew slowly, and had pale green leaves (Figures 3C–3E; Table S1). The leaf color can be attributed to a decrease in chlorophyll concentration (chlorophyll *a* + *b*) (Table S2). WT-like growth and leaf color were fully restored by expression, in the *pgrl1ab* background, of either *PGRL1A* or *PGRL1B*

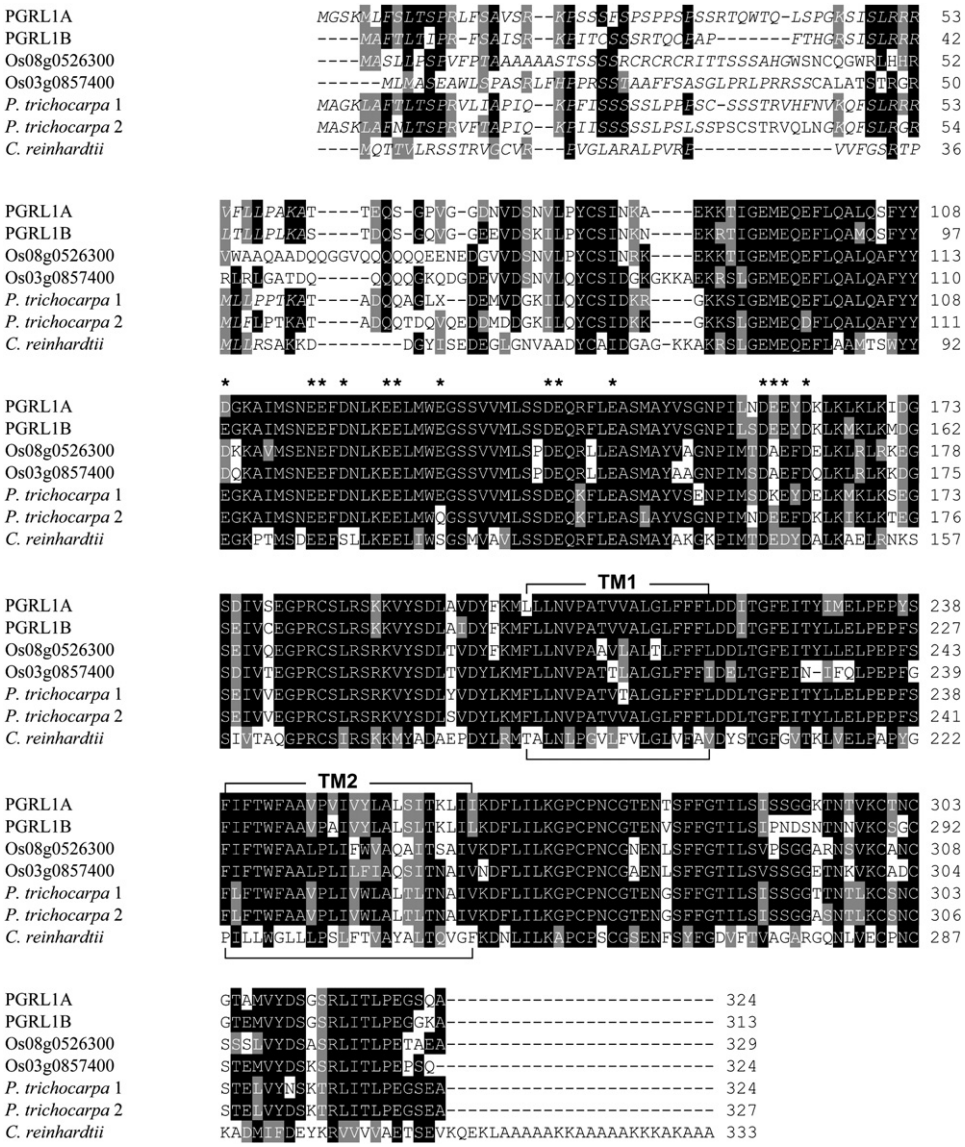

Figure 1. Sequence Alignment of the PGRL1 Proteins in *A. thaliana* and in Other Plant and Algal Species

The amino acid sequence of the *Arabidopsis* PGRL1A protein (At4g22890) was compared with the PGRL1B sequence (At4g11960) and with other related sequences from *Oryza sativa* (Os08g0526300, Os03g0857400), *Populus trichocarpa* (Protein IDs gw1.I.9237.1 and grail3.0018022902), and *Chlamydomonas reinhardtii* (Protein ID 183448). Black boxes indicate strictly conserved amino acids, and gray boxes closely related ones. Negatively charged amino acids are indicated by asterisks. Putative chloroplast transit peptides are indicated in italics, and the two transmembrane domains (TM1 and TM2) are highlighted. Note that the *Chlamydomonas* TM1 is predicted to contain N-terminally of the consensus TM in addition the amino acids "LRMT" (position 182–185).

under the control of the 35S promoter of Cauliflower Mosaic Virus, indicating that the two genes are functionally redundant.

Photosynthetic electron flow, measured on the basis of chlorophyll fluorescence, was altered at high light intensities (>400 $\mu E/m^2s$) in *pgrl1ab* plants, but not in either of the single mutants (Figure 4A; Table S3). The maximum quantum yield (F_V/F_M) in the *pgrl1ab* double mutant was normal, but it showed a moderate decrease in the effective quantum yield (Φ_{II}) and a slight increase in the fraction of Q_A (the primary electron acceptor of PSII) present in the reduced state (1-qP) (Table S3). These findings suggest that electron flow through PSII is unaltered but that a later electron transfer step is affected. Increasing light intensity leads to induction of NPQ in WT plants, but in the *pgrl1ab* mutant the degree of induction was substantially reduced. This is reminiscent of the behavior of the *pgr5* mutant, which is defective in Fd-dependent CEF (Munekage et al., 2002) (Figure 4B). An indirect method to measure CEF is to monitor NPQ induction during dark-to-light transition. In WT, NPQ was transiently induced within 1 min light (80 $\mu E/m^2s$) and relaxed within 2 min postinduction (Figure 4C), a behavior thought to be caused by a transient imbalance between generation (by CEF) and relaxation (by ATP synthase activity) of ΔpH

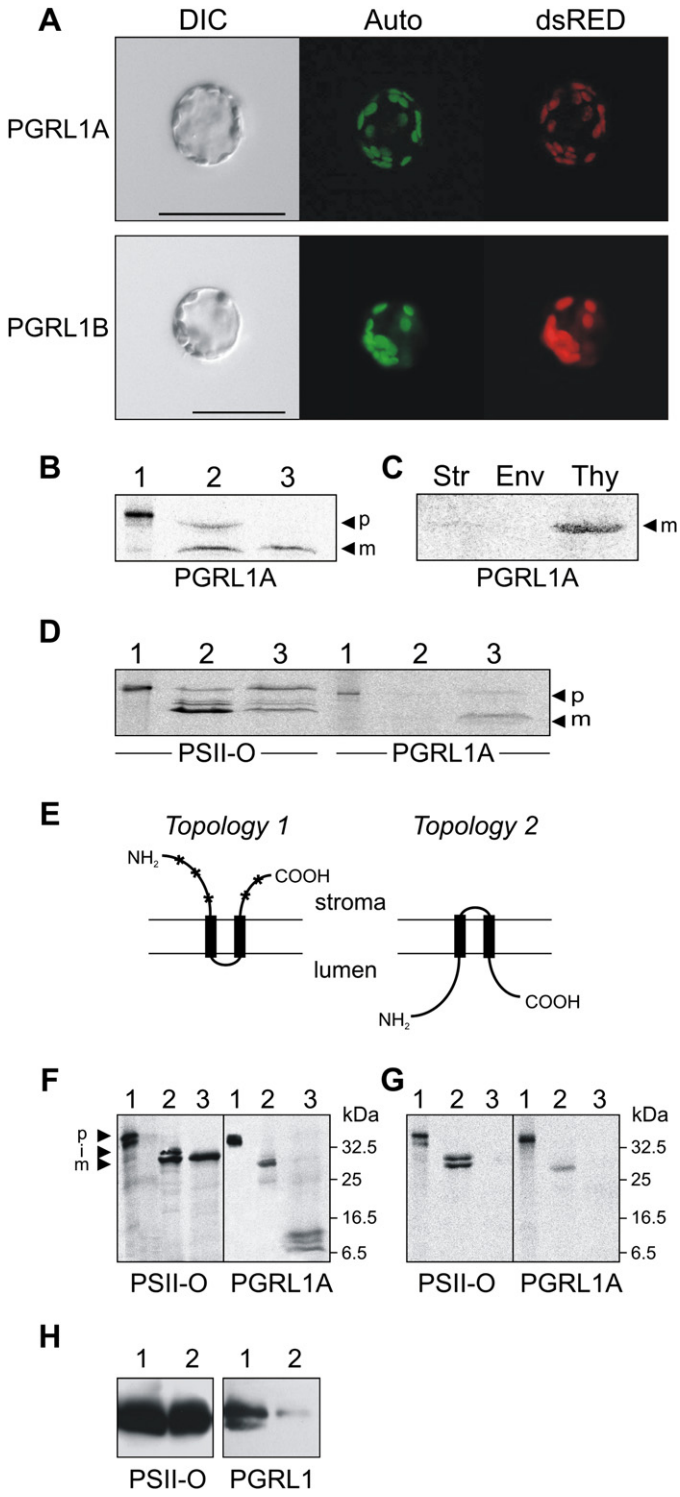

Figure 2. Subcellular Localization and Topology of PGRL1 Proteins

(A) Full-length PGRL1A- and PGRL1B-dsRED fusions were transiently introduced into *Arabidopsis* protoplasts by polyethylene glycol-mediated DNA uptake and analyzed using fluorescence microscopy (DIC, differential interference contrast image; Auto, chloroplasts revealed by chlorophyll autofluorescence; dsRED, fluorescence of the fusion protein). Scale bar = 50 μm.

(B) ^{35}S-labeled PGRL1A protein, translated in vitro (lane 1, 10% translation product) was incubated with isolated chloroplasts for 30 min at 25°C. Chloroplasts were recovered by centrifugation through 40% Percoll (lane 2) and incubated with thermolysin to remove adherent preproteins (lane 3) prior to SDS-PAGE. Proteins were visualized by autoradiography (p, precursor; m, mature protein).

(C) Chloroplasts were fractionated after protein import. Str, stroma; Env, envelope; Thy, thylakoids.

(D) After import of ^{35}S-labeled PGRL1A and PSII-O proteins (lane 1 was loaded with 10% of the translation product), chloroplasts were lysed and membranes were collected by centrifugation and treated with 6 M urea. Lane 2, solubilized proteins; lane 3, insoluble membrane fraction.

(E) Schematic representation of the two possible topologies of PGRL1. In contrast to the N and C termini, the loop between the two TMs lacks predicted trypsin cleavage sites (indicated by asterisks).

(F) Trypsin treatment of thylakoid membranes bearing PSII-O and PGRL1A labeled with ^{35}S. Pea chloroplasts corresponding to 20 μg of chlorophyll were incubated for 30 min with ^{35}S-labeled PSII-O and PGRL1A to permit uptake of the proteins. Intact chloroplasts were then recovered and treated with thermolysin to remove adherent preproteins (lane 2). Thylakoids were isolated and incubated with trypsin (10 μg/ml) (lane 3). Lane 1 represents 10% of the translation product. p, preprotein; i, intermediate; m, mature protein.

(G) Thylakoid membranes with incorporated ^{35}S-labeled PSII-O and PGRL1A were obtained as in (F). Thylakoids were treated first with β-dodecylmaltoside to release protein complexes from the membrane and then incubated with trypsin (10 μg/ml) (lane 3). Lanes 1 and 2 are as in (F).

(H) Immunoblotting with antisera specific for PSII-O or for the N-terminal portion of mature PGRL1 before (lane 1) and after (lane 2) treatment of thylakoid membranes with trypsin. In intact thylakoids only stroma-exposed polypeptides are accessible to trypsination.

Note that in the experiments shown in (B)–(D) and (F) and (G), PGRL1B behaves like PGRL1A (not shown). Details on import assays and topology determination are given in the Supplemental Experimental Procedures.

(Munekage et al., 2002). Both *pgrl1ab* and *pgr5* mutants exhibited a severe reduction in the rapid and transient induction of NPQ (Figure 4C), which is attributed to CEF around PSI during the reactivation of photosynthesis upon exposure to light (Munekage et al., 2002).

If indeed Fd-dependent CEF is affected in *pgrl1ab*, one would expect to see an effect on the oxidation state of the PSI reaction center (P_{700}) and on reduction of PQ, as in the case of the *pgr5* mutant (Munekage et al., 2002). The dependence of the P_{700} oxidation ratio (ΔA/ΔAmax) on light intensity in *pgrl1ab* plants, measured as absorbance changes at 820 nm, was indeed found to be very similar to that seen in the *pgr5* mutant, where the decrease in CEF is thought to lower the ATP/NADPH ratio during photosynthesis, leading to stromal overreduction and depletion of $NADP^+$, thus indirectly decreasing P_{700} oxidation by charge recombination (Munekage et al., 2002; Shikanai, 2007) (Figure 4D). To investigate the decrease in P_{700} oxidation observed in *pgrl1ab* and *pgr5* in more detail, the amount of photooxidizable P_{700} was measured as a function of the dark interval between two consecutive illuminations. In WT, very short dark periods ($\leq$5 ms) are sufficient to allow complete reduction of P_{700}^+, which can then be reoxidized during the subsequent light period.

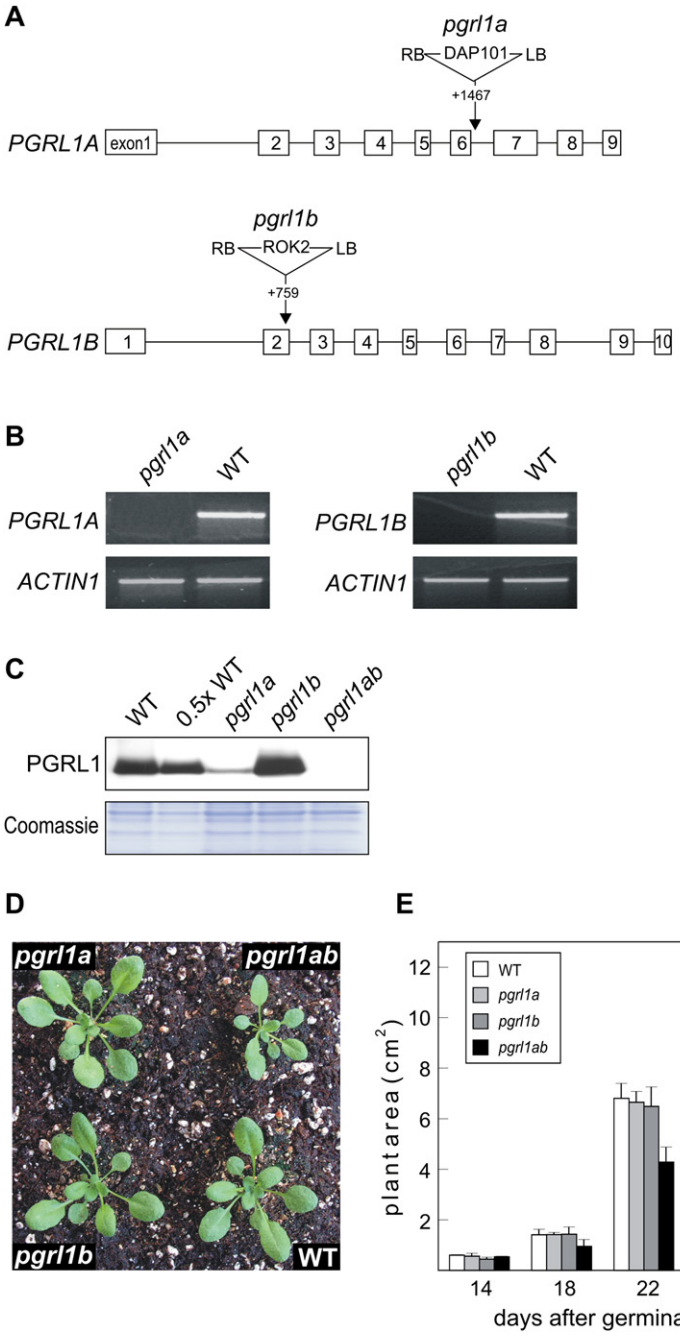

Figure 3. *pgrl1* Mutations and Their Effects on Transcript and Protein Accumulation and on Plant Development

(A) The translated parts of exons (boxes), as well as intron sequences (lines), are depicted. For each T-DNA mutant used in this study, the insertion site and the orientation of the T-DNA are indicated. The corresponding lines for *pgrl1a* were identified in the SAIL collection (SAIL_443E10) and for *pgrl1b* in the SALK T-DNA collection (SALK_059233). The T-DNA insertions are not drawn to scale.

(B) Effects of *pgrl1a* and *pgrl1b* mutations on transcript accumulation. Transcripts were detected by RT-PCR. Amplified amplicons were selected to lie 5′ to the insertion for *pgrl1a* and 3′ for *pgrl1b*. PCR products obtained after 40 cycles with gene-specific primers and control primers for the *ACTIN1* gene were analyzed on a 1% (w/v) agarose gel.

(C) Aliquots of thylakoid proteins corresponding to 3.5 μg of chlorophyll from wild-type (WT) and mutant plants were loaded in each lane (except lane 0.5× WT which contains the equivalent of 1.75 μg chlorophyll). Filters were immunolabelled with an antibody raised against the N-terminal part of mature PGRL1A. As loading control a Coomassie-stained replicate gel is shown in the lower panel.

(D) Phenotypes of 3-week-old WT plants, and *pgrl1a*, *pgrl1b*, and *pgrl1ab* mutants grown in the greenhouse.

(E) Growth kinetics of *pgrl1a*, *pgrl1b*, and *pgrl1ab* plants compared to WT. Twenty-four plants of each genotype were measured during the period from 14 to 26 days after germination. Mean values ± standard deviations (SDs; bars) are shown.

In contrast, in *pgrl1ab* and *pgr5* plants reoxidation of P_{700} in the light is slow ($t_{1/2}$ of ~50 ms) (Figures 4E and S1A), suggesting that, in the absence of PGRL1 or PGR5, the regeneration of PSI acceptors is impaired, i.e., a significant portion of the PSI acceptors remain reduced during the dark period.

pgrl1 Mutants and *pgr5* Mutants Are Similarly Affected in CEF

To assess electron transfer from Fd to PQ during CEF around PSI, Fd-dependent reduction of PQ was monitored in situ as an increase in chlorophyll fluorescence under low measuring light (Munekage et al., 2002) (Figure 4F). In WT, the addition of NADPH and Fd to ruptured chloroplasts induces a marked increase in chlorophyll fluorescence that reaches a plateau after 60 s. In this in situ assay NADPH is thought to transfer electrons to Fd via the reverse reaction of the Fd:$NADP^+$ reductase (FNR). In *pgrl1ab* plants, as in the *pgr5* mutant (Munekage et al., 2002), the increase in chlorophyll fluorescence reaches a markedly lower plateau compared to WT, suggesting that PGRL1 and PGR5 operate in the same pathway associated with Fd-dependent CEF. In the same assay, the *psad1-1* (Ihnatowicz et al., 2004) and *psae1-3* (Ihnatowicz et al., 2007) mutants, which both display a pronounced decrease in subunits forming the stromal part of PSI and both exhibit a severe impairment of PSI oxidation and a partial block in LEF, were examined. Both mutants exhibited an increased CEF efficiency compared to WT, as indicated by the fact that chlorophyll fluorescence reaches a higher plateau.

To measure the rates of CEF around PSI in intact leaves, the kinetics of P_{700} oxidation were followed after illumination with far-red light when PSII has a 10-fold lower turnover rate than PSI (Joliot and Joliot, 2005). In this intact-leaf assay, the relatively slow P_{700} oxidation observed in dark-adapted leaves is thought to signal the occurrence of CEF, whereas the fast P_{700} oxidation observed in light-adapted leaves should reflect the rate of LEF because the Calvin cycle is activated (Joliot and Joliot, 2005). Without preillumination, *pgrl1ab*, *pgr5*, and WT plants

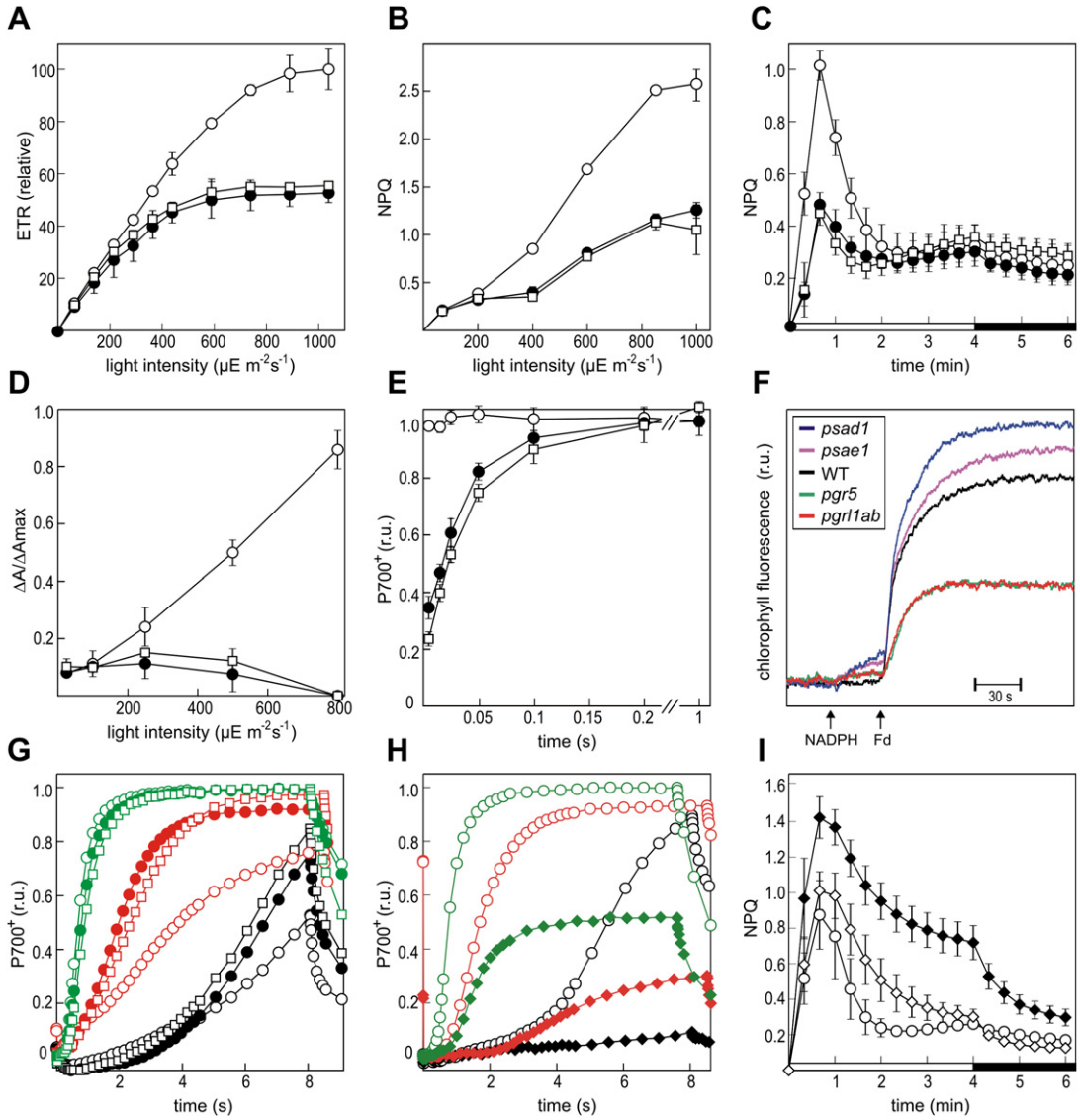

Figure 4. Characterization of Photosynthetic Electron Flow

(A–E) Average values ± SD (bars) of five different plants for WT are indicated as open circles, for *pgrl1ab* as filled circles, and for *pgr5* as squares. (F–H) Independent experiments on five different plants were performed, and representative results are shown.

(A) Dependence of the relative electron transport rate (ETR) on light intensity. ETR is represented as relative values of the maximum ETR in the WT (100%).

(B) Dependence of nonphotochemical quenching (NPQ) of chlorophyll fluorescence in leaves upon light intensity.

(C) Time courses of induction and relaxation of NPQ monitored during dark-to-light (80 μE/m^2s, white bar) transition. The 4 min light period (white bar) was followed by a 2 min dark period (black bar). Note that NPQ induction during the activation period of photosynthesis is thought to be caused by the transient acidification of the thylakoid lumen when CEF activity is higher than the activity of the ATP synthase.

(D) Dependence of the P_{700} oxidation ratio (ΔA/ΔAmax) on light intensity.

(E) P_{700} oxidation as a function of the dark interval (5 ms to 1 s) between two consecutive illuminations (see Figure S1A for original data). The level of P_{700} oxidation corresponds to the amount of P_{700} reduced during the dark period. Data are expressed as relative values.

(F) Quantification of CEF in situ. Increases in chlorophyll fluorescence were measured in ruptured chloroplasts under low measuring light (1 μE/m^2s), after the addition of NADPH and Fd. At this light intensity, the fluorescence level should predominately reflect the reduction of plastoquinone by cyclic electron transport from ferredoxin, not by PSII photochemistry (Munekage et al., 2002).

(G) Quantification of CEF in intact leaves. P_{700} oxidation was induced by illumination with far-red light (see Figure S1B for detailed data). Dark-adapted leaves from WT (open circles), *pgrl1ab* (filled circles), and *pgr5* (squares) plants were illuminated for different times with green light to induce LEF (black borders/filling, 0 s; red, 20 s), and P_{700} oxidation was recorded 200 ms after the green light was switched off. A 5 min exposure to green light, followed by 2 min in the dark, is indicated by green borders/filling. Data are expressed as relative values.

(H) Quantification of CEF in WT (open circles) and *psad1-1* mutant (filled diamonds) plants using the intact-leaf assay as in (G) (see Figure S1C for detailed data). Note that the *psae1-3* mutant behaved similarly to *psad1-1* (data not shown).

exhibited similar P_{700} oxidation kinetics, an observation that has previously been suggested to reflect similar abilities to perform CEF (Nandha et al., 2007). In leaves that were first illuminated for 5 min with green light to activate LEF, oxidation of P_{700} occurred as rapidly in *pgrl1ab* plants as in the *pgr5* mutant and in WT plants. These results imply that, under these conditions, LEF has replaced CEF with equal efficiency in all three genotypes (Figures 4G and S1B). However, after shorter periods of priming with green light, both *pgrl1ab* and *pgr5* showed faster P_{700} oxidation than WT, clearly implying that the CEF-to-LEF transition occurs more rapidly in the two mutants. In the same assay, P_{700} oxidation is suppressed in dark-adapted leaves of *psad1-1* (Figures 4H and S1C) and *psae1-3* (data not shown) mutants, indicating that they display increased rates of CEF. Because in *psad1-1* and *psae1-3* plants CEF around PSI appeared to be increased in both the in situ and the intact-leaf assay (Figures 4F and 4H), an increase in lumen acidification with concomitant enhancement of NPQ induction would be expected in the mutants. Previous measurements of NPQ, both under constant light and as a function of changing light intensity, have shown that plants with less PSI-D exhibit an increase in NPQ and in the size of the pool of xanthophyll cycle pigments (Haldrup et al., 2003; Ihnatowicz et al., 2004). Indeed, in both *psad1-1* and *psae1-3* plants, a dark-to-light transition provokes a more rapid and transient induction of NPQ than is observed in WT plants (Figure 4I). This indicates either that destabilization of the stromal ridge of PSI indirectly increases CEF as a regulatory response to the decrease in LEF, or that the altered structure of mutant PSI directly increases its affinity for components of CEF, resulting in a higher rate of CEF in the *psad1-1* and *psae1-3* mutants.

Taken together, both the intact-leaf assay and the in situ assay indicate that CEF is perturbed to similar extents in *pgrl1ab* and *pgr5* mutants. However, the relative severity of the CEF defect revealed by the two assays differs (Nandha et al., 2007; see Discussion section). In the *psad1-1* and *psae1-3* mutants, CEF appears to be increased.

PGRL1 Interacts with PGR5, PSI, FNR, and Cyt b_6/f

To investigate whether, in addition to their functional interaction, PGRL1 can also interact physically with PGR5, we employed split-ubiquitin and two-hybrid assays in yeast (Figures 5A and 5B), as described in the Supplemental Experimental Procedures. In the split-ubiquitin assay, PGRL1 and PGR5 interacted (Figure 5A). Because the topology of PGRL1 allows efficient protein-protein interaction only with the stroma-exposed N- and C-terminal loops (see Figure 2E), we infer that PGR5 must be located at the stromal face of the thylakoid membrane. The stromal exposure of PGR5 was indeed confirmed by protease protection assays (Figure S2). To identify further physical interactions between PGRL1 (or PGR5) and other thylakoid proteins thought to be involved in CEF around PSI, interaction studies were extended to Fd, PSI-D, Cyt b_6 (PetB), and the two FNR isoforms, FNR1 and FNR2. Whereas PGR5 interacts in yeast two-hybrid assays with Fd and in the split-ubiquitin assay with Cyt b_6, the PGRL1 protein interacts in the split-ubiquitin assay with Fd, PSI-D, Cyt b_6, FNR1, and FNR2 (Figures 5A and 5B), pointing to a central role for PGRL1 in multiple interactions between components of Fd-dependent CEF. To determine which of the two stroma-exposed loops of PGRL1 is responsible for the protein-protein interactions described above, additional yeast two-hybrid analyses were performed. Interaction between PGRL1 and Fd were found to require the C-terminal loop of the former (see "C-PGRL1" in Figure 5B). Binding between the individual loops and PGR5, the FNR isoforms, PSI-D, or Cyt b_6 could not be detected (data not shown), implying that both loops might be required for such interactions. The abundance of negatively charged amino acids in the N-terminal loop of PGRL1 (see Figure 1), however, indicates that the positively charged PGR5 protein (Munekage et al., 2002) might interact with this part of the mature PGRL1 protein.

PGRL1 Interacts In Planta with PSI and PGR5 But Is Not a Constitutive Subunit of Any Major Thylakoid Multiprotein Complex

The relationship between PGRL1 and other thylakoid proteins, in particular PGR5, was also studied using 2D gel methods. In the *pgrl1ab* mutant, the stability of the major thylakoid multiprotein complexes was not noticeably affected (Figure S3). Immunoblot analyses of total leaf proteins from photosynthetic mutants lacking PSII, PSI, Cyt b_6/f, or the chloroplast ATPase indicated that PGRL1 can accumulate independently of the major thylakoid protein complexes (Figure 5C). As in the *pgr5* mutant (Munekage et al., 2002), Cyt b_6/f and NDH complexes accumulate to WT levels in *pgrl1ab* plants, as indicated by immunoblot analyses of representative subunits (Figure 5D).

However, in the absence of PGRL1, no accumulation of PGR5 was observed, whereas PGR5 expression is not essential for accumulation of PGRL1 (Figure 5C). To probe the relationship between PGRL1 and PGR5 in more detail, thylakoid preparations from WT, *pgrl1ab*, and *pgr5* plants were immunoblotted and analyzed with antibodies specific for PGRL1 and PGR5 (Figures 5E). Whereas PGRL1 can stably accumulate in plants devoid of PGR5, no traces of the PGR5 protein could be detected in thylakoid preparations from plants lacking PGRL1. At the mRNA level, the accumulation of *PGR5* and *PGRL1* transcripts was not affected in *pgrl1ab* and *pgr5* plants, respectively (Table S1), indicating that the changes in protein abundance noted above occur at the translational or posttranslational level.

Although presence of PSI is not required for the stable accumulation of PGRL1 (see Figure 5C), the protein is found together with PGR5 in PSI preparations from WT plants (Figure 5E), indicating that the two proteins at least transiently associate with the PSI complex. This association, however, plays no role in stabilizing the PSI complex because absence of PGRL1 (or PGR5) has no effect on the composition of the

(I) NPQ induction in WT, *psad1-1*, and *psae1-3* plants. Transient increase and relaxation of NPQ were monitored as in (C) in the WT (open circles), *psad1-1* (filled diamonds), and *psae1-3* (open diamonds). Average values ± SD (bars) of five different plants for each genotype are shown.

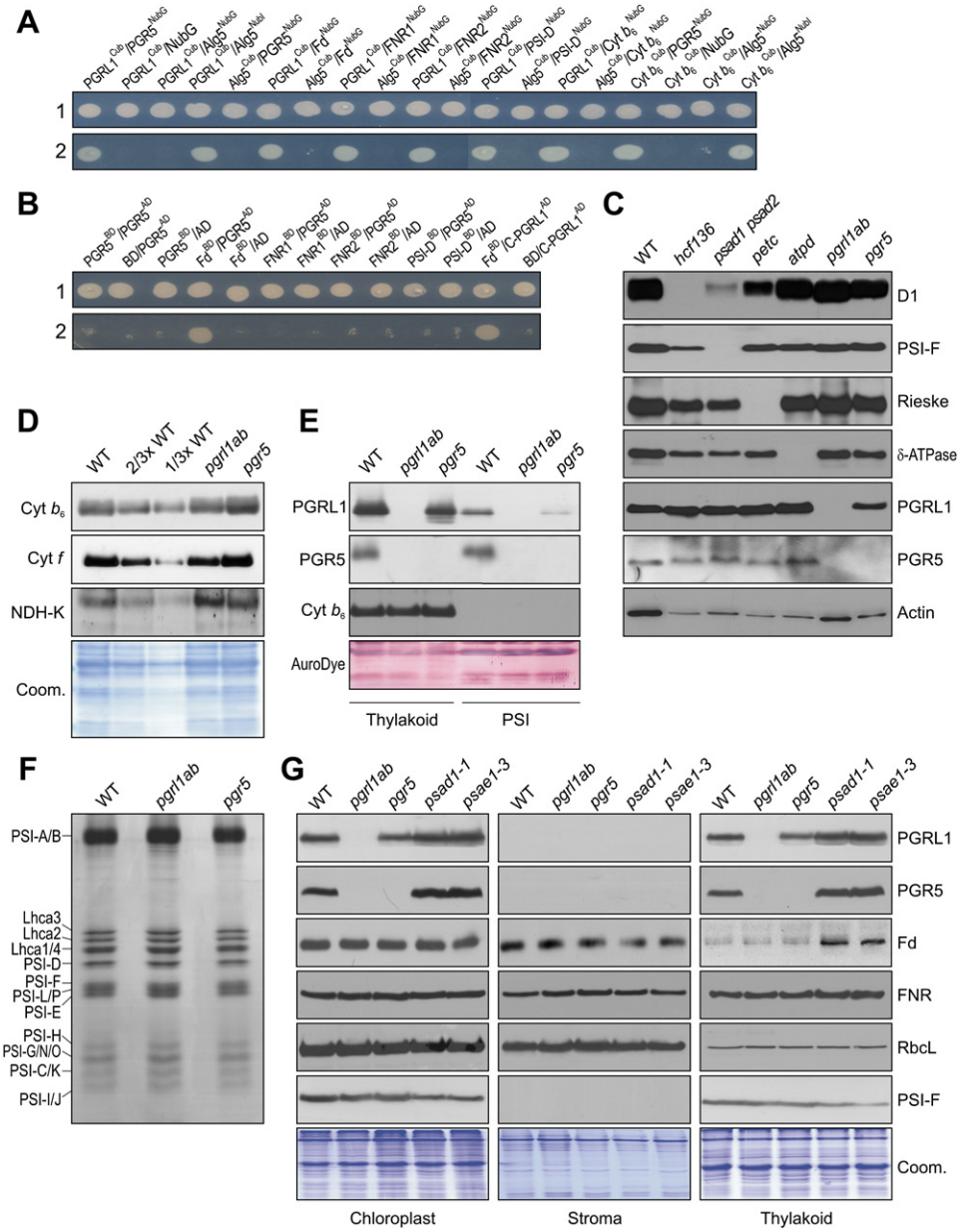

Figure 5. Characterization of the PGRL1 Protein and of Its Interactions

(A) Split-ubiquitin assays were performed employing fusions to the C- (Cub) and N- (NubG) terminal halves of ubiquitin. Alg5^{NubI}, the fusion of the unrelated ER membrane protein Alg5 to NubI (the WT Nub), was used as positive control. Negative controls were fusions of Alg5 to Cub or NubG (Alg5^{Cub} and Alg5^{NubG}), as well as the empty vector expressing soluble NubG. Additional negative controls are described in the Supplemental Experimental Procedures. Yeast colonies were first plated on permissive (1) and then on selective medium (2).

(B) Yeast two-hybrid assays were performed using the GAL4-based system. PGR5 was fused to the GAL4 activation domain (PGR5^{AD}) and its ability to form homo- and heterodimers was tested by employing PGR5, Fd, FNR1, FNR2, and PSI-D fused to the GAL4-binding domain (PGR5^{BD}, Fd^{BD}, FNR1^{BD}, FNR2^{BD}, PSI-D^{BD}). The Fd^{BD} protein fusion was also tested for interaction with the C-terminal loop of PGRL1 fused to the GAL4 activation domain (C-PGRL1^{AD}). Autoactivation was tested by cotransforming with the empty counterpart vector (AD or BD). Plating on permissive (1) and selective (2) media was done as described in the Supplemental Experimental Procedures.

(C) Immunoblot analysis of leaf proteins (corresponding to 8 μg of total protein) from WT, *pgrl1ab*, and *pgr5* mutants and mutants devoid of PSII (*hcf136*), PSI (*psad1 psad2*), Cyt b_6/f (*petc*), or the chloroplast ATPase (*atpd*). Antibodies specific for PGR5, PGRL1, and the respective thylakoid multiprotein complexes, or Actin as control, were used.

(D) Accumulation of subunits of the Cyt b_6/f and NDH complexes in WT, *pgrl1ab*, and *pgr5* mutant plants, detected by western analysis. Analyses were performed on thylakoid proteins using specific antibodies directed against Cyt b_6, Cyt *f*, or subunit K of the plastid NDH complex. Lower amounts of WT proteins were loaded in lanes 2/3× WT and 1/3× WT, as indicated. In the lower panel, a replicate gel stained with Coomassie blue (Coom.) is shown as loading control.

PSI complex or on the accumulation of its various subunits (Figure 5F).

Synthetic Phenotype of *pgrl1ab psad1-1* Triple Mutants

To clarify whether the abundance of putative components of CEF on the stromal side of PSI is changed in mutants with decreased (*prg5* and *pgrl1ab*) or increased (*psad1-1* and *psae1-3*) CEF rates, PGR5, PGRL1, Fd, and FNR were analyzed by western blotting of proteins isolated from total chloroplasts, stroma, or thylakoids (Figure 5G). Lack of PGR5 or PGRL1 has no marked effect on the abundance of Fd and FNR, although a slight increase in the stromal fraction of FNR can be seen. The increase in CEF in *psad1-1* and *psae1-3* is associated with increased levels of PGRL1 and PGR5, with a slight increase in the abundance of thylakoid-associated FNR, and with markedly increased amounts of Fd in the thylakoid fraction. Interestingly, Haldrup et al. (2003) found the amount of Fd in total protein extracts of *PsaD* antisense plants to be only slightly increased relative to WT, and in our hands Fd levels were not markedly altered in the total chloroplast preparations from *psad1-1* or *psae1-3* plants (Figure 5G), suggesting that the surplus protein might be associated with PGRL1-PGR5 and/or Cyt b_6/f (Zhang et al., 2001) or another thylakoid component.

The increase in levels of PGRL1 and PGR5, together with Fd and FNR associated with thylakoids, seen in *psad1-1* and *psae1-3* plants might indicate that their markedly increased rates of CEF (Figures 4F and 4H) are functionally linked to the rise in levels of the PGRL1-PGR5 complex. If this hypothesis is true, measurable consequences for plant performance would be expected if one deprives *psad1-1* or *psae1-3* plants of the ability rapidly to switch from LEF to CEF by introducing the *pgrl1ab* mutation, thereby removing the PGRL1-PGR5 complex. To this end, *pgrl1ab psad1-1* triple mutants were generated by crossing. The triple mutants indeed showed markedly decreased growth, very pale leaves, and a further impairment in photosynthesis (Figure 6; Table S3), implying that enhanced CEF, which requires formation of the PGRL1-PGR5 complex, helps to compensate for the photosynthetic lesion induced by the *psad1-1* mutation.

DISCUSSION

The mechanisms that regulate Fd-dependent CEF (or "CEF around PSI") are still unclear, but, in principle, there are two ways to shunt electrons from Fd back into PSI: (1) via the FQR-dependent pathway to PQ (reviewed in Shikanai, 2007) or (2) to Cyt b_6/f via FNR (Zhang et al., 2001; Joliot and Joliot, 2002; Kramer et al., 2004). A supercomplex comprising PSI, Cyt b_6/f, and Pc that is formed in response to changes in the stromal ATP concentration and operates to regulate the CEF/LEF ratio (Joliot and Joliot, 2002) so far could not be identified during proteomic studies (Breyton et al., 2006), but its existence cannot be excluded.

Although PGR5 does not contain a sequence motif that qualifies the protein to participate directly in CEF, the lower plateau of chlorophyll fluorescence during Fd-dependent reduction of PQ in situ and the drop in NPQ seen in *pgr5* mutants has lead to the suggestion that PGR5 plays a significant role in CEF around PSI (Munekage et al., 2002). Alternative approaches to the measurement of CEF that resolve the much faster chlorophyll fluorescence changes in vivo have, however, suggested that in *pgr5* mutants the maximum rate of CEF is only slightly affected (Nandha et al., 2007), implying that PGR5 instead plays a role in regulating the switch between LEF and CEF and that absence of PGR5 reduces the capability of CEF to compete for electrons with LEF. However, even if only minor changes in CEF occur in the absence of PGR5, the resulting alterations in the ATP/NADPH ratio should be sufficient to have substantial effects on ADP, P_i, and $NADP^+$ levels, restricting the availability of PSI electron acceptors and thereby regulating LEF (Kramer et al., 2004; Avenson et al., 2005).

Overall, two major questions regarding Fd-dependent CEF remain open. (1) Does PGR5 play a direct or indirect (regulatory) role? (2) Which protein (complex) receives electrons from Fd? To address these questions we have identified and functionally characterized the PGRL1 protein.

Functional and Physical Interaction of PGRL1 and PGR5

Our results indicate that PGRL1 and PGR5 interact both functionally and physically: the *pgrl1ab* and *pgr5* mutants show very similar growth behaviors (data not shown) and photosynthetic phenotypes; PGRL1 and PGR5 interact in yeast and copurify in PSI preparations; and accumulation of the peripheral PGR5 protein requires PGRL1 (but not vice versa). This suggests that PGR5, located at the stroma side of thylakoids (see Figure S2), is bound to the stroma-exposed domains of PGRL1 and that lack of PGRL1 prevents stable accumulation of PGR5. Because absence of PGR5 results in reduced accumulation of the PGRL1 protein, PGR5 may increase the stability of PGRL1. However, PGRL1 and PGR5 must work in concert to mediate

(E) Immunoblot analysis of thylakoid samples (equivalent to 3.5 μg chlorophyll) or PSI preparations (equivalent to 5 μg chlorophyll) from WT, *pgrl1ab*, and *pgr5* mutants, using antibodies specific for PGR5 or PGRL1. Cyt b_6 was used as a negative control for Cyt b_6/f contamination in PSI preparations and AuroDye staining as loading control.

(F) PSI subunit composition in WT, *pgrl1ab*, and *pgr5* mutant plants. Identical amounts of PSI complexes (equivalent to 5 μg chlorophyll) isolated from WT and mutant leaves were fractionated by SDS-PAGE (16% to 23% acrylamide gel) and visualized by Coomassie blue staining. Positions of subunits previously identified by immunodetection are indicated.

(G) Western analyses of stromal PSI-associated proteins putatively involved in CEF in WT and mutants with decreased (*pgrl1ab* and *pgr5*) or increased (*psad1-1* and *psae1-3*) CEF. Antibodies specific for PGRL1, PGR5, Fd, and FNR were used to probe protein samples from total chloroplasts, thylakoids, and stroma preparations. Lanes of chloroplast fractions correspond to 5 μg of chlorophyll. Stroma and thylakoid fractions were obtained after lysis and fractionation of chloroplasts corresponding to 5 μg of chlorophyll. Antibodies specific for the large subunit of Rubisco (RbcL) and PSI-F were used as controls for the purity of the fractions. As a loading control, a replicate gel was stained with Coomassie blue (Coom.).

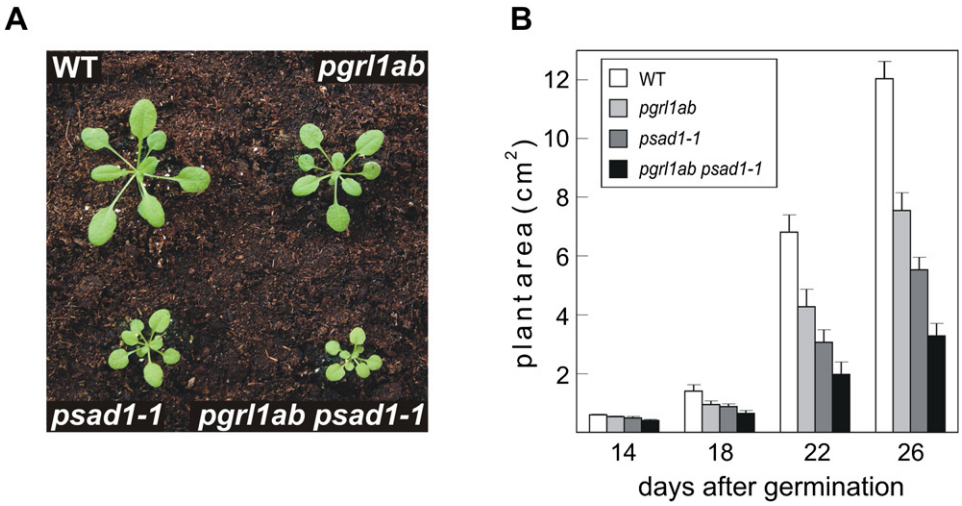

Figure 6. Phenotypes and Growth Kinetics of *pgrl1ab*, *psad1-1*, and *pgrl1ab psad1-1* and WT Plants

(A) Phenotype of 3-week-old mutant and WT plants grown in the greenhouse.

(B) Growth kinetics. Twenty-four plants of each genotype were measured during the period from 14 to 26 days after germination. Mean values ± standard deviations (SDs; bars) are shown.

efficient CEF around PSI: PGRL1 alone cannot support the process, as indicated by the *pgr5* mutant, in which decreased amounts of PGRL1 are still expressed (see Figures 5C and 5E) but a *pgrl1ab*-like CEF phenotype is nevertheless evident; on the other hand PGR5 cannot accumulate in the absence of PGRL1, as evident in the *pgrl1ab* mutant, implying at least a structural function for PGRL1.

A Model for the Role of PGRL1-PGR5 in Fd-Dependent CEF

PGRL1 exhibits a number of characteristics that are compatible with a role as a regulator or component of Fd-dependent CEF. (1) It is an integral thylakoid protein with two stroma-exposed domains, implying that it might be capable of interacting with stromal and/or stroma-exposed thylakoid proteins, as well as with other integral thylakoid proteins; (2) it indeed interacts in yeast with PSI, Fd, FNR, and Cyt b_6/f—all components known or suspected to be involved in Fd-dependent CEF; (3) it copurifies with PSI. Together with its functional and physical interaction with PGR5, which is already known to be involved in CEF around PSI, and the concomitant increase in CEF, PGRL1-PGR5, and thylakoid-associated levels of Fd and FNR in the *psad1-1* and *psae1-3* mutants, these findings allow us to propose a model for the function of the PGRL1-PGR5 complex in Fd-dependent CEF. In Figure 7, scenarios for the involvement of the PGRL1-PGR5 complex in LEF (Figure 7A) and CEF (Figure 7B) are shown. Two principal types of behavior of the PGRL1-PGR5 complex appear possible: the complex could be constitutively associated with PSI—which would argue for the occurrence of *LEF1* and *CEF3* or *CEF4* (see Figure 7). The copurification of PGRL1-PGR5 with PSI favors *LEF1*, but the accumulation of PGRL1-PGR5 in the absence of PSI (see Figure 5C) and the present lack of biochemical evidence for a Cyt b_6/f-PSI supercomplex clearly argue against *CEF3* and *CEF4*. The stability of the PGRL1-PGR5 complex in the absence of PSI or Cyt b_6/f makes it more likely that PGRL1-PGR5 can interact independently with each of the complexes, indicating that in vivo the variant *CEF1* or *CEF2* might operate. A further attractive feature of *CEF1* is its compatibility with previous findings reporting an association of FNR with Cyt b_6/f in spinach (Zhang et al., 2001) (see below).

Fd-Dependent CEF: Cyanobacteria versus Plants

Cyanobacteria possess no PGRL1 homolog and, unlike plant preparations, cyanobacterial Cyt b_6/f preparations lack the FNR complex (Zhang et al., 2001). This indicates that Fd-dependent CEF involving the PGRL1-PGR5-FNR-Fd complex (Figure 7B) might be restricted to eukaryotes, implying that CEF around PSI in cyanobacteria might depend on other proteins. In this respect it is interesting to note that the function of the PGRL1-PGR5 complex becomes limiting for plant performance under conditions where CEF is increased, as in the *psad1-1* and *psae1-3* mutants, for instance. In these genotypes the decreased abundance of subunits of the stromal face of PSI (Ihnatowicz et al., 2004, 2007) is associated with an increase in CEF and in the induction of NPQ (see Figures 4F, 4H, and 4I). The latter response is likely to downregulate PSII activity, thus adjusting the rate of LEF to accommodate the impairment of PSI activity in these genotypes (Haldrup et al., 2003; Ihnatowicz et al., 2004, 2007). In this context it can be concluded that the interaction between PGRL1 and PSI-D (see Figure 5A) is not essential for CEF in *Arabidopsis*. In contrast, CEF around PSI is not increased in cyanobacterial strains that lack PSI-E (Yu et al., 1993). This can only be explained by assuming that different mechanisms of Fd-dependent CEF operate in cyanobacteria and plants.

Does PGRL1-PGR5 Play a Direct or Indirect Role in CEF around PSI?

Based on our data, the PGRL1-PGR5 complex may either be essential for Fd-dependent CEF in plants or play a more indirect,

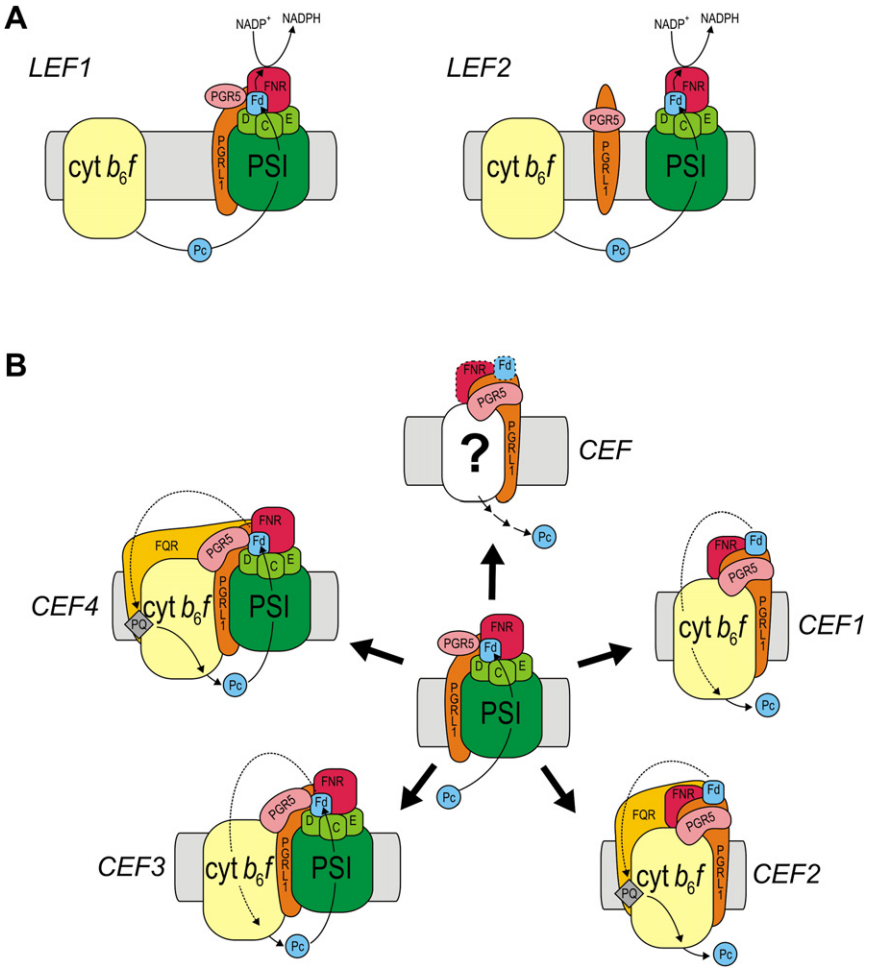

Figure 7. Schematic Model for the PGRL1/PGR5-Dependent Switch between CEF and LEF

(A) During LEF (continuous lines), electrons are transferred from Fd to $NADP^+$ via FNR. The PGRL1-PGR5 complex could be either associated with PSI (*LEF1*) or mobile (*LEF2*).

(B) During CEF, PGRL1-PGR5 could act either as a shuttle, possibly in complex with FNR and Fd (indicated by dotted lines), between PSI and another thylakoid protein with so far unclear identity (white filling highlighted with "?"; *CEF*), which might be Cyt b_6/f alone (*CEF1*) or the FQR together with Cyt b_6/f (*CEF2*), or as a direct linker between the two multiprotein complexes ("supercomplex"; *CEF3* and *CEF4*). Note that the inclusion of Cyt b_6/f in the CEF scenarios is based on the independent interaction of PGR5 and PGRL1 with Cyt b_6/f in yeast (see Figure 5A) and the copurification of FNR, another interactor of PGRL1, with Cyt b_6/f in flowering plants and not in cyanobacteria (Zhang et al., 2001), which so far also lack a PGRL1 homolog (see main text).

In simpler models PGRL1-PGR5 either would replace FNR (when not considering the interaction between PGRL1 and FNR, as detected in Figure 5A) or PGRL1-PGR5-FNR would represent the FQR itself.

regulatory role in this process. In the latter case, our model makes a number of predictions that can be experimentally tested. If PGRL1-PGR5 is a regulator rather than a component of CEF around PSI, as was suggested based on experiments with the *pgr5* mutant previously (Nandha et al., 2007), a basic Fd-dependent CEF mechanism—possibly conserved between cyanobacteria and plants—should exist and "spontaneous" interaction between its components should be possible (i.e., in the absence of PGRL1-PGR5). This would argue in favor of the scenario with a supercomplex (*CEF3* and *CEF4* in Figure 7B), the formation of which would be promoted (or accelerated) by PGRL1-PGR5. In case of reversible migration of a PGRL1-PGR5-FNR-Fd complex between PSI and Cyt b_6/f (*CEF1* and *CEF2* in Figure 7B), a regulatory but nonessential function of PGRL1-PGR5 in CEF would imply that the FNR-Fd complex could migrate to Cyt b_6/f without PGRL1-PGR5, albeit to a lesser extent or with altered kinetics, thus impairing the switch from LEF to CEF.

The Acceptor of Electrons from Fd in CEF: FQR or Cyt b_6/f ?

Because the FQR enzyme has not been identified yet, its possible interaction with the PGRL1-PGR5 complex could not be tested in this work. The interaction of both PGRL1 and PGR5 with Cyt b_6/f in yeast—in combination with the interaction of PGRL1 with FNR, which in turn has been reported to copurify with Cyt b_6/f (Zhang et al., 2001)—is compatible with the view that Cyt b_6/f accepts electrons from Fd mediated by the action of PGRL1 and PGR5. In this respect, it is possible that no distinct FQR enzyme exists, but that the FQR activity might result directly from the concerted action of PGRL1, PGR5, and FNR.

EXPERIMENTAL PROCEDURES

Plant Lines, Propagation, and Growth Measurement

Mutant lines were either obtained from the SAIL (Sessions et al., 2002) and SALK (Alonso et al., 2003) T-DNA mutant collections or from Toshiharu Shikanai (*pgr5* mutant; Munekage et al., 2002). Methods for plant propagation and for the measurement of their growth have been described elsewhere (Ihnatowicz et al., 2004, 2007).

Nucleic Acid Analysis

Arabidopsis DNA was isolated (Ihnatowicz et al., 2004), and T-DNA insertion junction sites were recovered by PCR using combinations of insertion- and gene-specific primers and sequenced.

Analyses of Chlorophyll Fluorescence and P_{700} Redox States

Five plants of each genotype were analyzed and average values and standard deviations were calculated. Photosynthetic electron transport and NPQ were measured as described previously (Munekage et al., 2002; Ihnatowicz et al., 2004). Changes in the redox state of P_{700} were measured by monitoring absorbance at 810 nm and 860 nm with a PAM 101/103 chlorophyll fluorometer (Walz) connected to a dual wavelength ED-P_{700}DW emitter-detector unit. Oxidized P_{700} (ΔA) was recorded during illumination with actinic white light

(from 70 to 800 μE/m^{2}s). The maximum content of oxidized P_{700} (ΔAmax) was recorded during illumination with far-red light (720 nm; 50 μE/m^{2}s). The P_{700} oxidation state was then calculated as (ΔA/ΔAmax).

CEF-to-LEF transitions were measured as P_{700} redox kinetics in intact leaves with a flash spectrophotometer as described before (Nandha et al., 2007). Actinic light driving LEF was provided by a green LED peaking at 520 nm, and P_{700} oxidation was measured at 820 nm (Breyton et al., 2006). P_{700} was specifically excited by far-red light and the maximum extent of P_{700}^+ was estimated from the kinetics of P_{700} oxidation as described (Joliot and Joliot, 2005).

The redox state of P_{700} was measured as a function of the dark period between consecutive illuminations. The variable dark interval between the two illuminations (2 ms to 1 min) is designed to permit reduction of P_{700}^+ and regeneration (oxidation) of PSI electron acceptors. After the dark period a short saturating pulse of light was applied to reoxidize P_{700}. The level of P_{700} reoxidation was then plotted as a function of the interval between the two illuminations.

In Situ Assay of Ferredoxin-Dependent Plastoquinone Reduction Activity

Ferredoxin-dependent plastoquinone reduction activity was measured in ruptured chloroplasts as described (Munekage et al., 2002) using 5 μM spinach ferredoxin (Sigma) and 0.25 mM NADPH.

In Vitro Transcription and Translation

The *PGRL1A* and *PGRL1B* cDNAs were cloned 3′ to the T7 promoter in the pGEM-T vector (Promega). mRNA was obtained by transcription with T7 RNA polymerase (MBI Fermentas Leon-Rot, Germany) and used for translation in wheat germ extracts (Wheat Germ Extract System, Promega, Madison, WI, USA) in the presence of ^{35}S-methionine. The *PSBO* construct was transcribed from the SP6 promoter, and proteins were synthesized in reticulocyte extracts (Flexi, Promega). All translation mixtures were centrifuged at 50,000 g (1 hr; 4°C) prior to import experiments.

Immunoblot Analyses and PGRL1-Specific Antiserum

Thylakoid or total chloroplast proteins or PSI complexes were prepared from 4-week-old *Arabidopsis* leaves, fractionated on an SDS-polyacrylamide gradient gel (8%–25% polyacrylamide), and transferred to poly(vinylidene difluoride) membranes (Ihnatowicz et al., 2004). Filters were then probed with antibodies specific for individual thylakoid proteins and signals were detected by enhanced chemiluminescence (Amersham Biosciences).

PGRL1-specific antibodies were raised against the N-terminal loop (aa 61 to 200; N-PGRL1) of PGRL1A. For this purpose the corresponding cDNA was cloned into pET151Topo (Invitrogen) and transformed into the BL21Star strain of *E. coli* for IPTG-induced protein expression following the manufacturer's instructions. The N-PGRL1 protein was purified by virtue of its His-Tag using Ni-NTA Agarose (QIAGEN) and injected into rabbits for antibody production.

PSI Complex Preparation and Thylakoid Protein Isolation

Thylakoid membranes were prepared as described (Ihnatowicz et al., 2004, 2007), washed twice with 5 mM EDTA (pH 7.8), centrifuged (5 min, 10,000 g, 4°C), and resuspended in double-distilled water. After solubilization with 2% (w/v) β-dodecyl maltoside for 10 min at 4°C, PSI isolation and subsequent fractionation by 16%–23% gradient SDS-PAGE were carried out as described (Ihnatowicz et al., 2007). Proteins were visualized by staining with colloidal Coomassie blue.

Supplemental Data

Supplemental Data include three figures, three tables, Supplemental Experimental Procedures, and Supplemental References and can be found with this article online at http://www.cell.com/cgi/content/full/132/2/273/DC1/.

ACKNOWLEDGMENTS

We thank the Deutsche Forschungsgemeinschaft (grant B8 of SFB-TR1) for support; Toshiharu Shikanai for providing PGR5-specific antibodies and *pgr5* mutant seeds; Peter Jahns for pigment analysis; Peter Westhoff for providing NDH-specific antibodies; Jörg Meurer for discussions; and Paul Hardy for critical comments on the manuscript.

Received: August 30, 2007
Revised: November 13, 2007
Accepted: December 20, 2007
Published: January 24, 2008

REFERENCES

Allen, J.F. (2003). Cyclic, pseudocyclic and noncyclic photophosphorylation: new links in the chain. Trends Plant Sci. *8*, 15–19.

Alonso, J.M., Stepanova, A.N., Leisse, T.J., Kim, C.J., Chen, H., Shinn, P., Stevenson, D.K., Zimmerman, J., Barajas, P., Cheuk, R., et al. (2003). Genome-wide insertional mutagenesis of *Arabidopsis thaliana*. Science *301*, 653–657.

Asada, K., Heber, U., and Schreiber, U. (1993). Electron flow to the intersystem chain from stromal components and cyclic electron flow in maize chloroplasts, as detected in intact leaves by monitoring redox change of P700 and chlorophyll fluorescence. Plant Cell Physiol. *34*, 39–50.

Avenson, T.J., Cruz, J.A., Kanazawa, A., and Kramer, D.M. (2005). Regulating the proton budget of higher plant photosynthesis. Proc. Natl. Acad. Sci. USA *102*, 9709–9713.

Bendall, D.S., and Manasse, R.S. (1995). Cyclic photophosphorylation and electron transport. Biochim. Biophys. Acta *1229*, 23–38.

Biehl, A., Richly, E., Noutsos, C., Salamini, F., and Leister, D. (2005). Analysis of 101 nuclear transcriptomes reveals 23 distinct regulons and their relationship to metabolism, chromosomal gene distribution and co-ordination of nuclear and plastid gene expression. Gene *344*, 33–41.

Breyton, C., Nandha, B., Johnson, G.N., Joliot, P., and Finazzi, G. (2006). Redox modulation of cyclic electron flow around photosystem I in C3 plants. Biochemistry *45*, 13465–13475.

Burrows, P.A., Sazanov, L.A., Svab, Z., Maliga, P., and Nixon, P.J. (1998). Identification of a functional respiratory complex in chloroplasts through analysis of tobacco mutants containing disrupted plastid *ndh* genes. EMBO J. *17*, 868–876.

Clarke, J.E., and Johnson, G.N. (2001). *In vivo* temperature dependence of cyclic and pseudocyclic electron transport in barley. Planta *212*, 808–816.

Cleland, R.E., and Bendall, D.S. (1992). Photosystem I cyclic electron transport: measurement of ferredoxin-plastoquinone reductase activity. Photosynth. Res. *34*, 409–418.

Finazzi, G., Furia, A., Barbagallo, R.P., and Forti, G. (1999). State transitions, cyclic and linear electron transport and photophosphorylation in *Chlamydomonas reinhardtii*. Biochim. Biophys. Acta *1413*, 117–129.

Golding, A.J., and Johnson, G.N. (2003). Down-regulation of linear and activation of cyclic electron transport during drought. Planta *218*, 107–114.

Golding, A.J., Finazzi, G., and Johnson, G.N. (2004). Reduction of the thylakoid electron transport chain by stromal reductants - evidence for activation of cyclic electron transport upon dark adaptation or under drought. Planta *220*, 356–363.

Haldrup, A., Lunde, C., and Scheller, H.V. (2003). *Arabidopsis thaliana* plants lacking the PSI-D subunit of photosystem I suffer severe photoinhibition, have unstable photosystem I complexes, and altered redox homeostasis in the chloroplast stroma. J. Biol. Chem. *278*, 33276–33283.

Harbinson, J., and Foyer, C.H. (1991). Relationships between the efficiencies of photosystems I and II and stromal redox state in CO_2-free air: evidence for cyclic electron flow in vivo. Plant Physiol. *97*, 41–49.

Havaux, M., Greppin, H., and Strasser, R.J. (1991). Functioning of photosystem I and photosystem II in pea leaves exposed to heat stress in the presence or absence of light - analysis using in-vivo fluorescence, absorbency, oxygen and photoacoustic measurements. Planta *186*, 88–98.

Havaux, M., Rumeau, D., and Ducruet, J.M. (2005). Probing the FQR and NDH activities involved in cyclic electron transport around photosystem I by the 'afterglow' luminescence. Biochim. Biophys. Acta *1709*, 203–213.

Herbert, S.K., Fork, D.C., and Malkin, S. (1990). Photoacoustic measurements in vivo of energy storage by cyclic electron flow in algae and higher plants. Plant Physiol. *94*, 926–934.

Ihnatowicz, A., Pesaresi, P., Varotto, C., Richly, E., Schneider, A., Jahns, P., Salamini, F., and Leister, D. (2004). Mutants for photosystem I subunit D of *Arabidopsis thaliana*: effects on photosynthesis, photosystem I stability and expression of nuclear genes for chloroplast functions. Plant J. *37*, 839–852.

Ihnatowicz, A., Pesaresi, P., and Leister, D. (2007). The E subunit of photosystem I is not essential for linear electron flow and photoautotrophic growth in *Arabidopsis thaliana*. Planta *226*, 889–895.

Joet, T., Cournac, L., Peltier, G., and Havaux, M. (2002). Cyclic electron flow around photosystem I in C_3 plants. In vivo control by the redox state of chloroplasts and involvement of the NADH-dehydrogenase complex. Plant Physiol. *128*, 760–769.

Joliot, P., Beal, D., and Joliot, A. (2004). Cyclic electron flow under saturating excitation of dark-adapted Arabidopsis leaves. Biochim. Biophys. Acta *1656*, 166–176.

Joliot, P., and Joliot, A. (2002). Cyclic electron transfer in plant leaf. Proc. Natl. Acad. Sci. USA *99*, 10209–10214.

Joliot, P., and Joliot, A. (2005). Quantification of cyclic and linear flows in plants. Proc. Natl. Acad. Sci. USA *102*, 4913–4918.

Joliot, P., and Joliot, A. (2006). Cyclic electron flow in C3 plants. Biochim. Biophys. Acta *1757*, 362–368.

Kramer, D.M., Avenson, T.J., and Edwards, G.E. (2004). Dynamic flexibility in the light reactions of photosynthesis governed by both electron and proton transfer reactions. Trends Plant Sci. *9*, 349–357.

Kurisu, G., Zhang, H., Smith, J.L., and Cramer, W.A. (2003). Structure of the cytochrome b_6f complex of oxygenic photosynthesis: tuning the cavity. Science *302*, 1009–1014.

Mi, H., Endo, T., Schreiber, U., Ogawa, T., and Asada, K. (1994). NAD(P)H dehydrogenase-dependent cyclic electron flow around photosystem I in the cyanobacterium *Synechocystis* PCC 6803 - a study of dark-starved cells and spheroplasts. Plant Cell Physiol. *35*, 163–173.

Mi, H.L., Endo, T., Ogawa, T., and Asada, K. (1995). Thylakoid membrane-bound, NADPH-specific pyridine nucleotide dehydrogenase complex mediates cyclic electron transport in the cyanobacterium *Synechocystis* sp PCC 68038. Plant Cell Physiol. *36*, 661–668.

Moss, D.A., and Bendall, D.S. (1984). Cyclic electron transport in chloroplasts: the Q-Cycle and the site of action of antimycin. Biochim. Biophys. Acta *767*, 389–395.

Munekage, Y., Hojo, M., Meurer, J., Endo, T., Tasaka, M., and Shikanai, T. (2002). PGR5 is involved in cyclic electron flow around photosystem I and is essential for photoprotection in *Arabidopsis*. Cell *110*, 361–371.

Munekage, Y., Hashimoto, M., Miyake, C., Tomizawa, K., Endo, T., Tasaka, M., and Shikanai, T. (2004). Cyclic electron flow around photosystem I is essential for photosynthesis. Nature *429*, 579–582.

Nandha, B., Finazzi, G., Joliot, P., Haid, S., and Johnson, G. (2007). The role of PGR5 in the redox poising of photosynthetic electron transport. Biochim. Biophys. Acta *1767*, 1252–1259.

Niyogi, K.K. (1999). PHOTOPROTECTION REVISITED: Genetic and molecular approaches. Annu. Rev. Plant Physiol. Plant Mol. Biol. *50*, 333–359.

Okegawa, Y., Tsuyama, M., Kobayashi, Y., and Shikanai, T. (2005). The *pgr1* mutation in the Rieske subunit of the cytochrome b_6f complex does not affect PGR5-dependent cyclic electron transport around photosystem I. J. Biol. Chem. *280*, 28332–28336.

Ravenel, J., Peltier, G., and Havaux, M. (1994). The cyclic electron pathways around photosystem I in *Chlamydomonas reinhardtii* as determined in-vivo by photoacoustic measurements of energy storage. Planta *193*, 251–259.

Rumeau, D., Becuwe-Linka, N., Beyly, A., Louwagie, M., Garin, J., and Peltier, G. (2005). New subunits NDH-M, -N, and -O, encoded by nuclear genes, are essential for plastid Ndh complex functioning in higher plants. Plant Cell *17*, 219–232.

Sessions, A., Burke, E., Presting, G., Aux, G., McElver, J., Patton, D., Dietrich, B., Ho, P., Bacwaden, J., Ko, C., et al. (2002). A high-throughput Arabidopsis reverse genetics system. Plant Cell *14*, 2985–2994.

Shikanai, T. (2007). Cyclic electron transport around photosystem I: genetic approaches. Annu. Rev. Plant Biol. *58*, 199–217.

Stroebel, D., Choquet, Y., Popot, J.L., and Picot, D. (2003). An atypical haem in the cytochrome b_6f complex. Nature *426*, 413–418.

Takabayashi, A., Kishine, M., Asada, K., Endo, T., and Sato, F. (2005). Differential use of two cyclic electron flows around photosystem I for driving CO_2-concentration mechanism in C_4 photosynthesis. Proc. Natl. Acad. Sci. USA *102*, 16898–16903.

Vallon, O., Bulte, L., Dainese, P., Olive, J., Bassi, R., and Wollman, F.A. (1991). Lateral redistribution of cytochrome b_6/f complexes along thylakoid membranes upon state transitions. Proc. Natl. Acad. Sci. USA *88*, 8262–8266.

Yu, L., Zhao, J., Muhlenhoff, U., Bryant, D.A., and Golbeck, J.H. (1993). PsaE is required for in vivo cyclice electron flow around photosystem I in the cyanobacterium *Synechococcus* sp. PCC 7002. Plant Physiol. *103*, 171–180.

Zhang, H., Whitelegge, J.P., and Cramer, W.A. (2001). Ferredoxin:$NADP^+$ oxidoreductase is a subunit of the chloroplast cytochrome b_6f complex. J. Biol. Chem. *276*, 38159–38165.

Accession Numbers

Nucleotide and protein sequences for PGRL1A and PGRL1B are available at the TAIR (AT4G22890 and AT4G11960), NCBI (NM_118418 and NM_117266), and UniProt (O82738 and Q9SZ61) databases.